BULLETIN OF THE ASTRONOMICAL INSTITUTES OF THE NETHERLANDS

1959 SEPTEMBER 26 VOLUME XIV NUMBER 492

COMMUNICATIONS FROM THE NETHERLANDS FOUNDATION FOR RADIO ASTRONOMY AND THE OBSERVATORY AT LEIDEN

NEUTRAL HYDROGEN IN M33 AND M101

BY LOUISE VOLDERS

The 21-cm emission from the two Sc nebulae M33 and M101 was observed with the 25-metre telescope at Dwingeloo. Intensity-velocity profiles at different positions in the nebulae were measured (Figures 1 and 2). The radial velocity of the centre of M33 with respect to the local standard of rest is -176 ± 2 km/sec, that of M101 is $+253 \pm 3$ km/sec. From the integrated profiles the density distribution of neutral hydrogen was computed (Tables 8 and 10). The maximum velocity of rotation is 102 km/sec for M33 and 176 km/sec for M101 (Tables 11 and 12). The model line profiles (dashed curves in Figures 1 and 2) are based on these rotation data and the density distribution. Distances of 630 c kpc for M33 and 2600 c kpc for M101 were used, c being an unknown correction factor to the present distance scale. The total mass of atomic hydrogen in M33 is $0.99 \times 10^9 c^2 M_\odot$, or 0.055 c times the total mass of the galaxy ($18 \times 10^9 c\, M_\odot$). The hydrogen mass of M101 is $2.98 \times 10^9 c^2 M_\odot$, or 0.021 c times the total mass $140 \times 10^9 c\, M_\odot$. The mass-luminosity ratio is 11 c^{-1} for M33 and 13 c^{-1} for M101.

1. *Method of observation*

The study of the Andromeda nebula in the 21-cm line with the 25-metre radiotelescope at Dwingeloo (VAN DE HULST, RAIMOND and VAN WOERDEN 1957, below called I) was followed by observations of other extragalactic systems. Preliminary results on M33 have been published (RAIMOND and VOLDERS 1957). The observations reported here were made during the months November and December, 1957, and January, 1958. The observing time was 190 hours for M33 and 240 hours for M101. Observations of M32 are reported in the following paper (WENTZEL and VAN WOERDEN 1959). Observations of five other systems are still in progress and will be discussed at a later date. Survey lists as of summer 1958 may be found elsewhere (VOLDERS and VAN DE HULST 1959; VAN DE HULST 1959).

The 21-cm receiver, designed and built by Ir C. A. MULLER, can be used with different bandwidths over a wide frequency interval. For this programme the bandwidth was 150 kc/s = 32 km/sec. The normal mode of operation gives an automatic comparison with two equally wide channels 1.08 Mc/s at either side of the measuring channel. One or the other or both comparison channels may be used.

The antenna pattern is supposed to be circularly symmetric. The width between half-power points is 0°.57. See Figure 1 in I.

The intensities to be measured are even smaller than in the Andromeda nebula. In order to obtain a good accuracy we adopted the same method as was used for the observations of M31. The telescope was set during 15 minutes on a selected point in the nebula, 15 minutes on a comparison field, again 15 minutes on the measuring point, and again 15 minutes on the comparison field. The comparison fields were chosen at a "safe" distance from the nebula. The average readings during the 15-minute intervals were obtained by eye estimate, discarding the first few minutes (the time constant was 54 sec). Then the systematic difference between nebula and comparison field was computed. Whenever galactic hydrogen line radiation in the measuring band might be suspected, two different comparison fields were used.

Figures 1a and 2a show sketches of the nebulae. The observed points on M33 are at intervals of 0.25 degrees along the major and minor axes. Mostly, the comparison fields V_1 and V_2 were used; closer pairs of comparison fields were used for $x = +1, +2, +3$ and $+4$, since this part of the nebula is nearly

CONTENTS

FIGURE 1

M33

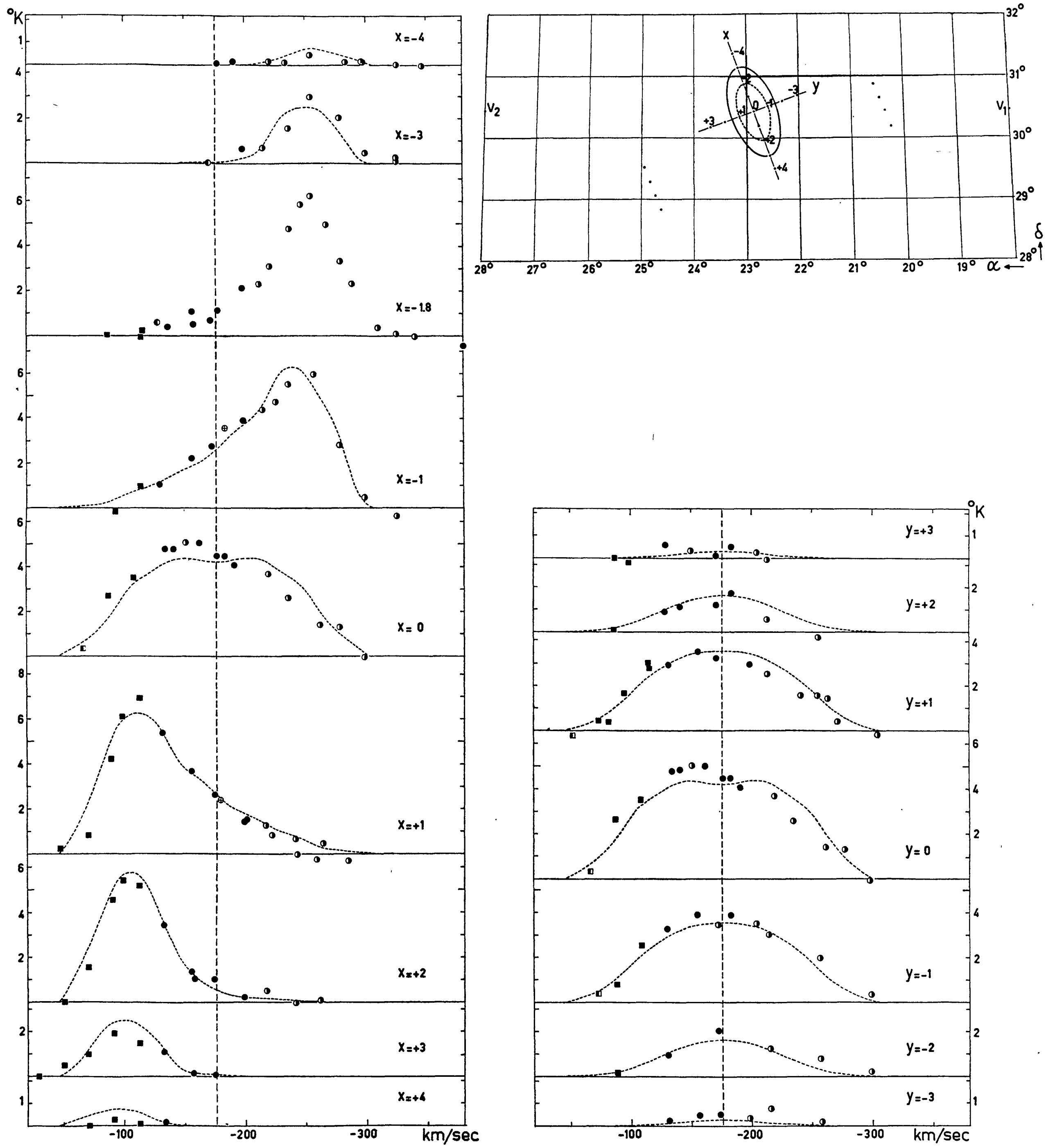

a. Sketch of M33 with observed points and comparison fields.

b. Observations (circles and squares) and computed model line profiles (dashed curves).

TABLE 2

Observations of M33; all velocities (in km/sec) are negative.

$x = -4$, $y = 0$, $\alpha = 23°.25$, $\delta = 31°.38$

$-V$	T
347	0.0
326	0.0
298	0.1
297	0.2
284	0.2
255	0.5
234	0.1
220	0.2
191	0.2
178	0.1

$x = -3$, $y = 0$, $\alpha = 23°.16$, $\delta = 31°.15$

$-V$	T
326	0.1
326	0.3
300	0.5
279	2.1
255	3.0
237	1.6
216	0.7
199	0.7
170	0.0

$x = -1.8$, $y = 0$, $\alpha = 23°.06$, $\delta = 30°.87$

$-V$	T
381	−0.4
340	0.0
325	0.1
310	0.4
289	2.3
279	3.3
268	5.0
254	6.2
246	5.9
237	4.8
221	3.1
212	2.3
198	2.1
179	1.1
171	0.7
158	0.5
156	1.1
136	0.4
128	0.6
115	0.2
114	0.0
87	0.0

$x = -1$, $y = 0$, $\alpha = 22°.96$, $\delta = 30°.68$

$-V$	T
325	−0.4
299	0.5
278	2.8
256	6.0
236	5.5
225	4.8
214	4.4
198	3.9
183	3.2
172	2.8
156	2.2
130	1.0
114	1.0
93	−0.2

$x = +1$, $y = 0$, $\alpha = 22°.76$, $\delta = 30°.20$

$-V$	T
285	−0.3
264	0.5
259	−0.2
242	0.0
241	0.7
221	0.8
216	1.3
200	1.6
199	1.4
179	2.4
174	2.6
155	3.7
132	5.4
112	7.0
99	6.1
89	4.2
70	0.8
47	0.2

$x = +2$, $y = 0$, $\alpha = 22°.66$, $\delta = 29°.97$

$-V$	T
261	0.1
241	0.0
217	0.5
199	0.2
174	1.0
158	1.1
156	1.4
132	3.4
113	5.2
99	5.4
90	4.6
70	1.6
48	0.2

$x = +3$, $y = 0$, $\alpha = 22°.56$, $\delta = 29°.73$

$-V$	T
175	0.1
156	0.2
132	1.1
113	1.5
91	2.0
70	1.0
50	0.5
29	0.0

$x = +4$, $y = 0$, $\alpha = 22°.47$, $\delta = 29°.50$

$-V$	T
134	0.2
113	0.1
92	0.3
71	0.0

$x = 0$, $y = -3$, $\alpha = 22°.04$, $\delta = 30°.70$

$-V$	T
258	0.2
216	0.8
198	0.3
174	0.5
156	0.5
132	0.2

$x = 0$, $y = -2$, $\alpha = 22°.32$, $\delta = 30°.61$

$-V$	T
300	0.2
257	0.8
215	1.2
173	2.0
131	1.0
88	0.2

$x = 0$, $y = -1$, $\alpha = 22°.59$, $\delta = 30°.53$

$-V$	T
299	0.4
257	2.0
215	3.0
204	3.5
183	3.9
172	3.4
156	3.9
130	3.3
109	0.5
88	0.8
73	0.4

$x = 0$, $y = 0$, $\alpha = 22°.86$, $\delta = 30°.44$

$-V$	T
298	−0.1
277	1.3
262	1.4
235	2.6
219	3.6
191	4.1
183	4.4
176	4.5
162	5.0
151	5.1
141	4.8
134	4.8
108	3.5
87	2.7
66	0.3

$x = 0$, $y = +1$, $\alpha = 23°.13$, $\delta = 30°.35$

$-V$	T
304	−0.2
276	0.4
263	1.4
255	1.6
241	1.6
213	2.5
199	3.0
170	3.2
155	3.5
131	2.9
116	2.8
114	3.0
95	1.7
82	0.4
73	0.4
52	−0.2

$x = 0$, $y = +2$, $\alpha = 23°.41$, $\delta = 30°.27$

$-V$	T
255	−0.2
213	0.6
183	1.7
171	1.2
141	1.1
128	0.9
86	0.1

$x = 0$, $y = +3$, $\alpha = 23°.68$, $\delta = 30°.18$

$-V$	T
213	−0.1
204	0.2
183	0.5
171	0.1
150	0.3
129	0.6
99	−0.2
87	0.0

FIGURE 2

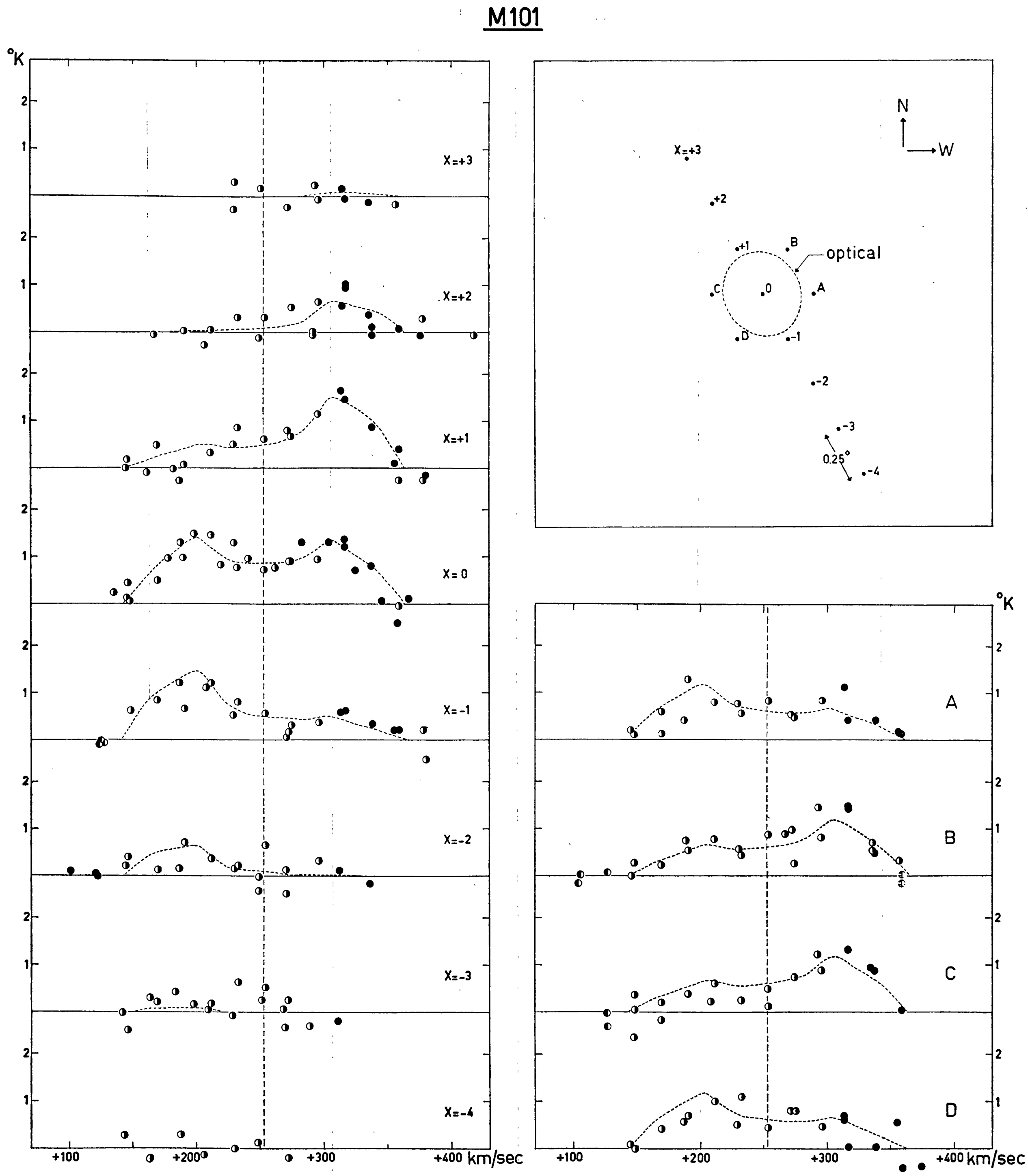

a. Sketch of M101 with observed points.
b. Observations (circles) and computed model line profiles (dashed curves).

TABLE 3

Observations of M101; all velocities (in km/sec) are positive.

$x = +3$, $y = 0$, $\alpha = 211^\circ.08$, $\delta = 55^\circ.20$

V	T
230	0.3
230	−0.3
251	0.2
272	−0.2
293	0.2
296	−0.1
314	0.2
317	0.0
335	−0.1
357	−0.2

B

$x = +0.50$, $y = -0.87$, $\alpha = 210^\circ.21$, $\delta = 54^\circ.77$

V	T
104	−0.2
106	0.0
127	0.1
146	0.0
148	0.3
169	0.2
189	0.8
190	0.6
211	0.8
231	0.7
233	0.4
254	0.9
267	0.9
273	1.0
275	0.2
293	1.4
296	0.8
317	1.4
317	1.5
336	0.7
336	0.5
338	0.5
357	0.3
359	0.0
360	−0.2

$x = +2$, $y = 0$, $\alpha = 210^\circ.86$, $\delta = 54^\circ.98$

V	T
167	0.0
190	0.0
207	−0.3
212	0.1
233	0.3
250	−0.1
254	0.3
275	0.5
292	0.0
292	−0.1
296	0.6
315	0.6
317	1.0
317	1.0
336	0.4
338	−0.1
338	0.1
359	0.1
376	−0.1
378	0.3
418	−0.1

$x = -3$, $y = 0$, $\alpha = 209^\circ.80$, $\delta = 53^\circ.90$

V	T
142	0.0
146	−0.4
164	0.3
170	0.2
184	0.5
191	0.2
209	0.0
212	0.2
228	−0.1
233	0.6
251	0.2
254	0.5
269	0.1
270	−0.3
272	0.3
290	−0.3
312	−0.2

$x = +1$, $y = 0$, $\alpha = 210^\circ.65$, $\delta = 54^\circ.77$

V	T
145	0.0
146	0.2
161	−0.1
169	0.5
183	0.0
187	−0.3
191	0.1
212	0.3
229	0.5
233	0.9
254	0.6
272	0.8
275	0.7
296	1.2
314	1.6
317	1.5
338	0.9
356	0.1
359	−0.2
359	0.4
378	−0.2
381	−0.1

D

$x = -0.50$, $y = +0.87$, $\alpha = 210^\circ.65$, $\delta = 54^\circ.33$

V	T
145	0.1
148	0.0
170	0.4
187	0.6
191	0.7
212	1.0
229	0.5
233	1.1
254	0.4
271	0.8
275	0.8
296	0.5
314	0.6
314	0.7
317	0.0
338	0.0
356	0.6
360	−0.4
375	−0.4

$x = 0$, $y = 0$, $\alpha = 210^\circ.43$, $\delta = 54^\circ.55$

V	T
135	0.2
145	0.0
148	0.0
156	0.4
170	0.1
177	0.9
188	0.1
190	0.0
198	1.5
211	0.0
220	0.8
230	0.2
232	0.0
241	0.9
253	0.1
262	0.8
273	0.0
274	0.1
283	1.3
295	0.3
304	1.3
316	0.1
316	0.1
325	0.7
338	0.2
346	0.1
359	0.1
359	0.0
367	0.1

$x = -4$, $y = 0$, $\alpha = 209^\circ.58$, $\delta = 53^\circ.68$

V	T
143	0.3
164	−0.2
164	−0.2
188	0.3
206	−0.1
230	0.0
248	0.1
272	−0.2

$x = -1$, $y = 0$, $\alpha = 210^\circ.21$, $\delta = 54^\circ.33$

V	T
124	−0.1
125	0.0
128	−0.1
149	0.6
170	0.8
187	1.2
191	0.7
208	1.1
212	1.2
229	0.5
233	0.8
254	0.6
271	0.1
273	0.2
275	0.3
296	0.4
313	0.6
317	0.6
338	0.3
356	0.2
360	0.2
378	0.2
381	−0.4

A

$x = -0.50$, $y = -0.87$, $\alpha = 210^\circ.00$, $\delta = 54^\circ.55$

V	T
145	0.2
148	0.1
170	0.1
170	0.6
187	0.4
190	1.3
211	0.8
230	0.8
232	0.6
254	0.8
272	0.5
274	0.5
296	0.8
314	1.1
316	0.4
338	0.4
356	0.2
359	0.1

$x = -2$, $y = 0$, $\alpha = 210^\circ.00$, $\delta = 54^\circ.11$

V	T
101	0.1
120	0.1
122	0.0
144	0.2
146	0.4
170	0.1
186	0.2
191	0.7
212	0.4
228	0.2
233	0.2
249	0.0
254	−0.3
254	0.7
270	0.1
271	−0.4
296	0.3
313	0.1
336	−0.2

C

$x = +0.50$, $y = +0.87$, $\alpha = 210^\circ.86$, $\delta = 54^\circ.55$

V	T
127	−0.3
127	0.0
148	−0.5
148	0.4
148	0.0
169	−0.2
170	0.2
190	0.4
208	0.2
211	0.6
232	0.2
254	0.1
254	0.5
274	0.7
293	1.2
296	0.9
317	1.3
335	1.0
338	0.9
359	0.0

stationary with respect to the local standard of rest. M101 was observed at the centre and at 6 points around it at a distance of 0°.25. From these measurements the direction of the major axis could be derived, and the points along the major axis, $x = \pm 2$, $x = \pm 3$ and $x = -4$ were observed later.

The *positions* were computed and set on the α and δ scales of the telescope with an accuracy of 0°.01. The guiding accuracy was better than at the time of the observations of M31: even when there was a strong wind, the position of the telescope was in good accordance with the position of the pilot. Thus, positioning errors are probably smaller than 0°.03. Errors of 0°.05 may have happened, but were very exceptional. Whenever the elevation was lower than 30°, the position of the telescope was corrected for refraction and bending of the telescope mast, using data by WESTERHOUT (1958). Observations of the radio sources Cas A, Cyg A and Vir A resulted in an estimated correction for positional errors caused by deviations of the radio axis from the pilot position. This correction was of some importance in only two measurements of M33, in which the positional correction rose to 0°.03 in δ. The corresponding temperature corrections, computed on the basis of the model nebula (Section 7), were 0.1 and 0.3 °K; these have been applied in Table 2 and Figure 1.

The *frequencies* were set with an accuracy better than 10 kc/s and were reduced to velocities with respect to the local standard of rest using the tables of MACRAE and WESTERHOUT (1956).

The unit of *intensity* is a degree Kelvin. We tried to bring the intensity scale in accordance with that defined by MULLER and WESTERHOUT (1957) by setting the condition that the top-intensity of the profile at $l = 50°$, $b = 0°$, measured with the Dwingeloo telescope and 40 kc/s bandwidth, should be 108 °K. We assume in the present paper that these temperatures are not antenna temperatures, as they were incorrectly called in *B.A.N.* No. 480 (I), but weighted averages of the brightness temperature in the full beam. The "full beam" may be defined, for instance, in the manner of *B.A.N.* No. 472, as the part of the antenna pattern enclosed within a circle of diameter 5 times the half-power diameter, or 2°.8, but the definition does not seem critical. Actual antenna temperatures are lower than these temperatures by perhaps 20 percent due to spillover. Precise data concerning the intensity calibrations of the Dwingeloo measurements will be published later.

The average sensitivity in the November-December period was only 1% less than in January. Furthermore, the measurements were corrected for the variations of the sensitivity with frequency. This systematic variation was measured; the corrections to be applied were found by interpolation from Table 1. Here f is the frequency of the second local oscillator and V' is the velocity component in the line of sight, not corrected for the motions of the Sun and Earth.

Extinction was neglected as it remained smaller than 2%.

TABLE 1

f (Mc/s)	V' (km/sec)	corr.	f (Mc/s)	V' (km/sec)	corr.
33.5	+ 584	+ 10%	36.5	− 49	0%
34.0	+ 479	+ 6	37.0	− 154	0
34.5	+ 373	+ 3	37.5	− 260	+ 1
35.0	+ 268	+ 2	38.0	− 365	+ 4
35.5	+ 162	+ 1	38.5	− 471	+ 7
36.0	+ 57	+ 0.5	39.0	− 576	+ 11

2. *Observational results*

Tables 2 and 3 give the intensity values obtained after the corrections mentioned above had been applied. They are plotted against the radial velocities relative to the local standard of rest in Figures 1b and 2b. The different symbols in these figures have the following meanings:

Black dots: two comparison channels have been used, one comparison field.

Black-white dots: one comparison channel has been used, one comparison field.

Open circles with cross: the radio-axis correction has been applied.

Squares: measurements with two comparison fields.

The theoretical accuracy of the intensities indicated by the different symbols is given on page 4 of the M31 article (I). The empirical values for the mean error μ of a 12-minute reading, determined from the statistics of the measurements, are as follows:

		number of points	μ	$0.80\,\mu$
M33	●	53	0.18 °K	0.14 °K
	◐ ◑	71	0.16	0.13
M101	●	56	0.22	0.17
	◐ ◑	167	0.17	0.14

The last column gives the mean errors expressed in terms of antenna temperature, assuming 20 per cent spillover. These values are in good agreement with the theoretical value of 0.15 °K.

In the reduction of the measurements with two comparison fields the assumption was made that the

FIGURE 3

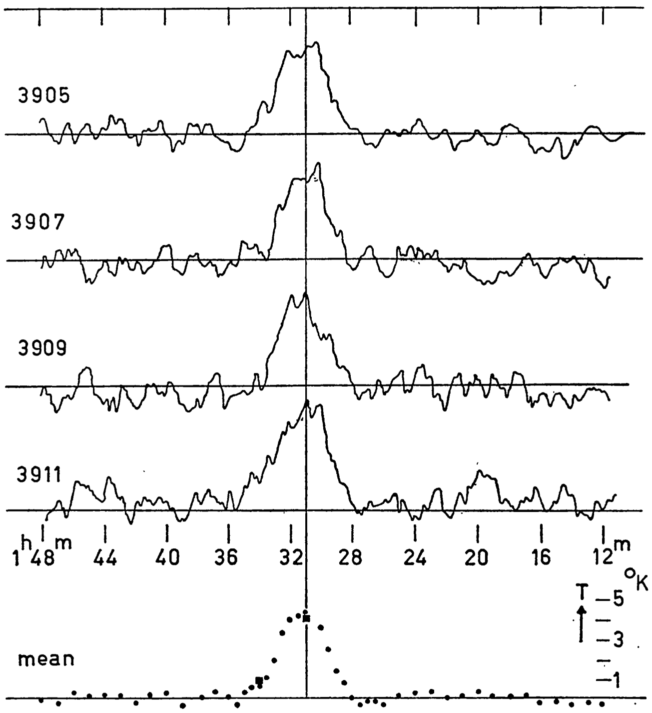

Four drift curves and their mean at $\delta = 30°17'$ and $V = -148$ km/sec with respect to L.S.R. The squares are obtained by interpolation from Figure 1b.

galactic foreground in the measured field is exactly the average of that in the two comparison fields. The errors introduced by this assumption cannot be very large as we found no systematic difference in any pair of comparison fields, and the random differences were always smaller than 0.25 °K.

Prompted by the Harvard observations (DIETER 1958) we checked our results by the method of drift curves. Figure 3 shows four drift curves and their mean at $\delta = +30°17'$ and $V = -148$ km/sec with respect to the local standard of rest. By taking 1-minute averages of the 4 curves, a mean error $0.80\,\mu = 0.24$ °K could be attained, in good agreement with the theoretical value of 0.26 °K. The squares at the points where the beam crosses the major and minor axes indicate the values found by interpolation from Figure 1b and demonstrate the consistency of these two series of measurements.

As a further check on the absence of radiation in the comparison fields differential measurements were made between the comparison field of M31 and V_1 of M33. This resulted in a difference $V_{M31} - V_{M33} = +0.1 \pm 0.1$ °K in the frequency range corresponding to velocities $+150$ to $+300$ km/sec. The comparison field V, which was used for nearly all measurements of M101, was compared with a field V' chosen symmetrically with respect to the centre of M101. The measured difference was $V - V' = 0.0 \pm 0.1$ °K.

3. *Optical data.*

Table 4 gives the most important optical data concerning both nebulae.

TABLE 4

	M33	ref	M101	ref
type of nebula	Sc		Sc	
co-ordinates centre	$\alpha = 22°.86$		$\alpha = 210°.43$	
(1958.0)	$\delta = 30°.44$		$\delta = 54°.55$	
position angle major axis	20°	1	30°	2
inclination angle i	33°	1	63°	2
radial velocity of the	−190 km/sec	3	+260 km/sec	3
centre, reduced to L.S.R.	−168 km/sec	1		
	−176 km/sec	2	+253 km/sec	2
distance	630 c kpc	5	2600 c kpc	6
dimensions	$83' \times 53'$	7	$28' \times 28'$	4,7
m_{pg}	$6^m.19$	7	$8^m.20$	7
apparent distance modulus	$24^m.1$	8	$27^m.1$	9

References to Table 4:

1) MAYALL and ALLER 1942, *Ap. J.* **95**, 5.
2) Present paper.
3) HUMASON, MAYALL and SANDAGE 1956, *A. J.* **61**, 97.
4) HOLMBERG 1950, *Medd. Lund Ser.* II, No 128.
5) From the observations of cepheids BAADE (unpublished) found the same distance modulus for M31 and M33. For this reason we have adopted here the distance SCHMIDT (*B.A.N.* **14**, 17 (No. 480), 1957) used for M31.
6) On account of distances calculated by HOLMBERG (reference 4, Table 10) we suppose M101 to have about the same distance as M81, 2600 kpc (SANDAGE, *A. J.* **59**, 181, 1954).
7) HOLMBERG 1958, *Lund Medd. Ser.* II, No. 136.
8) BAADE (private communication to Prof. OORT).
9) SANDAGE 1954, *A. J.* **59**, 181.

In the further reduction we require the position of the major axis and the inclination angle of M101. At first sight, M101 seems to lie in a plane perpendicular to the line of sight. However, by experimenting with oblique projection to make it look round, we found within a few degrees accuracy $i = 63°$; the position angle of the major axis was 30°. Observations of the 21-cm line at six points around the centre (the points A, B, $+1$, C, D, -1 in Figure 2) gave an independent determination of this position angle. An asymmetry measure was defined for these points as $d =$ average T in velocity interval 153 to 233 km/sec minus average T in interval 273 to 353 km/sec. The values for the six points are $100\,d = 3, 45, 92, 78, -28, -53$; by plotting them against position angle and fitting a sine curve, we found for the position angle of the major axis $\psi = 30° \pm 9°$ (m.e.).

4. *General formulae*

We want to find the hydrogen density distribution, rotation law and mass of the nebulae. The following assumptions are made:
1) the hydrogen is concentrated near one plane,
2) there is circular symmetry. This assumption will be temporarily replaced by the assumption of circular symmetry in each half of the nebula in the computation of $N(a)$, Tables 7 and 8.
3) the motion is along perfectly circular orbits.
Further the following symbols are introduced. Where possible, they have been chosen in agreement with paper I.

n_H = number density of hydrogen atoms in ground state (1S)
(a, φ, z) = cylindrical co-ordinates in nebula; z perpendicular to plane of nebula and $\varphi = 0$ on semi major-axis that has $V > 0$.

$N(a) = \int_{-\infty}^{\infty} n_H dz.$

i = inclination angle = angle between plane of nebula and line of sight.
$\Theta_{rot}(a)$ = circular velocity at distance a from centre.
$V(a) = \Theta_{rot}(a) \cos i$ = maximum observed velocity component at this distance.
$V(a, \varphi) = V(a) \cos \varphi$ = radial velocity relative to the centre of the nebula.
V_n = radial velocity of centre of nebula relative to the local standard of rest. $V(a, \varphi) + V_n$ = abscissa of Figures 1 and 2.
T = observed brightness temperature averaged over full antenna beam with the antenna pattern as weighting function.
(x, y) = rectangular co-ordinates of centre of beam on sky; (0,0) = centre of nebula.
$\theta = \sqrt{\{(x - a\cos\varphi)^2 + (y - a \sin i \sin \varphi)^2\}}$ = distance on sky between arbitrary point and centre of beam (Figure 4);
$f(\theta)$ = antenna pattern normalized by $f(0) = 1$ and taken 0 for $\theta > 0^\circ.75$ [1]).
$\Omega' = \int_0^{\infty} 2\pi\theta f(\theta)\, d\theta$. With the unit of $0^\circ.25$ for x, y, a and θ, used in the numerical computation, the value is $\Omega' = 5.50$ [1]).
ρ = half the distance between two successive rings in the model nebula.
m_H = mass of the hydrogen atom.

FIGURE 4

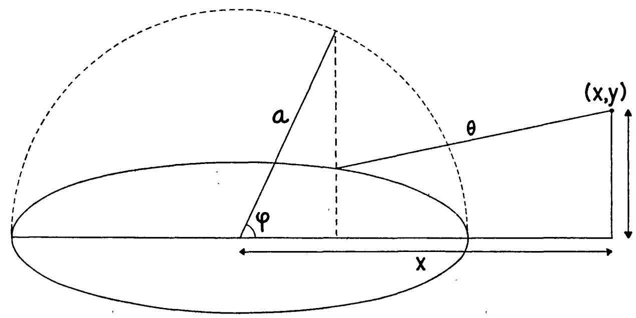

Geometrical quantities

The basic relation for any position of the antenna beam is [2])

$$\frac{1}{\Omega'}\int_0^{\infty}\int_0^{2\pi} N(a) f(\theta)\, a\, da\, d\varphi = 5.91 \times 10^{-4} \int_{-\infty}^{\infty} T\, dV, \quad (1)$$

which, upon introducing

$$J(x,y) = 5.91 \sin i \times 10^{-4} \int_{-\infty}^{\infty} T\, dV \quad (2)$$

and performing the integration over φ, becomes:

$$\int_0^{\infty} N(a) f_{xy}(a)\, da = J(x,y), \quad (3)$$

where

$$f_{xy}(a) = \frac{a \sin i}{\Omega'} \int_0^{2\pi} f(\theta)\, d\varphi. \quad (4)$$

Additional functions may be introduced by choosing variable limits of integration.

$$J(x, y; V_1) = 5.91 \sin i \times 10^{-4} \int_{V_1}^{\infty} T\, dV \quad (5)$$

$$f_{xy}(a, \varphi_1) = \frac{a \sin i}{\Omega'} \int_{-\varphi_1}^{\varphi_1} f(\theta)\, d\varphi. \quad (6)$$

[1]) The omission of any antenna sensitivity outside the main beam does not introduce an error but is in keeping with the definition of the temperature scale explained on page 328. The reduction is correct if the line radiation received from outside the main beam can be neglected. Alternatively, we might have used antenna temperatures $T_a = 0.80\ T$ (assuming 20 per cent spillover) and have integrated over the entire sphere, so that Ω' would be replaced by $\Omega = 5.50/0.80 = 6.88$. Eq. 1 shows that the results obtained would then be identical with those given below. The notations Ω and Ω' are in agreement with those given on page 97 of *B.A.N.* No. 472.

[2]) In I, eq. 10, the numerical factor is 6.0×10^{-4}. A more exact calculation of the transition probability A, which is now found to be 2.87×10^{-15} sec^{-1}, resulted in the more correct value 5.91×10^{-4}.

We then obtain the equation

$$\int_0^\infty N(a)\, f_{xy}(a, \varphi_1)\, da = J(x, y;\, V_1), \tag{7}$$

where $\varphi_1 = 0$ for $V_1 \geq V(a)$,

$$\cos\varphi_1 = \frac{V_1}{V(a)} \text{ for } |V_1| < V(a), \tag{8}$$

$$\varphi_1 = \pi \text{ for } V_1 \leq -V(a).$$

Eqs (5) — (8) define the line profile in the absence of the line broadening effects caused by random cloud motions and instrumental bandwidth. On the simple assumption that these effects have a rectangular distribution, i.e. that they spread a peak at velocity V evenly over the range of velocities from $V - {}^1/_2\,\Delta V$ to $V + {}^1/_2\,\Delta V$, the line profile is given by

$$5.91 \sin i \times 10^{-4}\, T(x,y;V_1) = \frac{J(x,y;V_1 - {}^1/_2\,\Delta V) - J(x,y;V_1 + {}^1/_2\,\Delta V)}{\Delta V}. \tag{9}$$

In order to make the solution for the density distribution feasible, we consider the hydrogen in the nebula to be concentrated in narrow rings at $a = 2\rho$, 4ρ, 6ρ, ... and a point at $a = 0$.
Upon defining

$$q_0 = \frac{2}{\rho^2}\int_0^\rho N(a)\, a\, da,$$
$$q_a = \frac{1}{2\rho\, a}\int_{a-\rho}^{a+\rho} N(a)\, a\, da, \tag{10}$$

equation (3) is replaced by the set of linear equations

$$J(x,y) = \frac{\pi\rho^2 \sin i}{\Omega'}\, q_0 f(\sqrt{x^2+y^2}) + \Sigma\, q_a f_{xy}(a)\,, \tag{11}$$

and, correspondingly, eq. (7) by

$$J(x,y;\,V_1) = \frac{\pi\rho^2 \sin i}{\Omega'}\, q_0 f(\sqrt{x^2+y^2}) + \Sigma\, q_a f_{xy}(a,\varphi_1)\,. \tag{12}$$

The total amount of atomic hydrogen in the nebula is

$$M_H = m_H \int_0^\infty N(a)\, 2\pi a\, da = 2\pi m_H\left(\frac{\rho^2}{2} q_0 + 2\rho\,\Sigma\, a q_a\right). \tag{13}$$

The total mass of the nebula may be written in the form

$$M = k\,\frac{\Theta_{rot}^2 R}{G}, \tag{14}$$

where R is the distance from the centre, Θ_{rot} is the velocity with which the material at this distance is rotating, G is the gravitation constant, 6.67×10^{-8} dyne cm^2 g^{-2}, and k is a numerical factor introduced by this relation. It is clear that k approaches 1 when R is large. In order to have an idea about the value of k for different values of R, calculations were made for the final model of the Galactic System (SCHMIDT 1956) and the Andromeda-Nebula model (SCHMIDT 1957). Figure 5 shows the results, together with the k-curve for the non-homogeneous, composite spheroid SCHMIDT used in the M31-model. The first two curves cross the level $k = 1$ because these models also contain non-composite spheroids, whose density falls sharply off to zero.

We can see from Figure 5 that, putting $k = 1$ and calculating M for the largest R for which any hydrogen is found (for M31 this is 27.5 kpc) an accuracy of 10% is very probably attained.

FIGURE 5

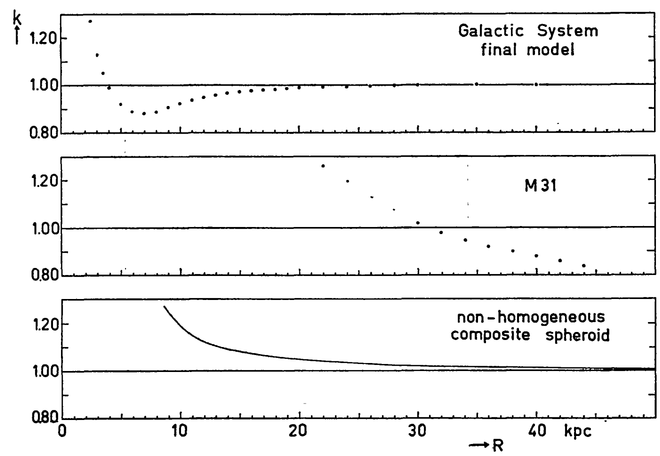

Curves giving values of k (see eq. (14)) for SCHMIDT's models of the Galactic System and M31 and for a non-homogeneous, composite spheroid. Abscissae are distances from the centre.

5. *Radial velocity of the centre*

The radial velocity of the centre of gravity of the nebulae was determined from the line profiles by two slightly different methods.

a) By requiring that observed points on the major axis at equal distance from the centre give symmetrical profiles. All ordinates of one profile were multiplied by a common factor to give the profiles approximately the same height. This factor, which was always 1 for M101, allowed for asymmetries in the mass distribution. One profile was then drawn on transparent paper, was put with inverse velocity scale on the other one and shifted sideways until the best coincidence was found. The radial velocity of the centre, V_n, then is half the sum of coinciding velocities of the two profiles.

b) By trying to fit the model profiles to the observed profiles.

TABLE 5
Radial velocity of M33

method *a*				method *b*			
field pair	multiplier North	multiplier South	V_n ± m.e. (km/sec)	field $x(\frac{1}{4}°)$	V_n ± m.e. (km/sec)	field $y(\frac{1}{4}°)$	V_n ± m.e. (km/sec)
± 1	1	1	− 179 ± 3	+ 1	− 177 ± 2	+ 1	− 171 ± 2
± 3	1	1.3	− 178 ± 2	+ 2	− 178 ± 2	+ 2	− 178 ± 7
± 4	1	1	− 180 ± 5	+ 3	− 173 ± 4	+ 3	− 151 ± 25
				− 1	− 175 ± 2	− 1	− 178 ± 4
				− 3	− 184 ± 4	− 2	− 183 ± 7
						− 3	− 188 ± 25
	weighted mean		− 178 ± 1	weighted mean	− 177 ± 1	weighted mean	− 174 ± 2

TABLE 6
Radial velocity of M101

method *a*		method *b*	
field pair	V_n ± m.e. (km/sec)	field	V_n ± m.e. (km/sec)
0	+ 252 ± 2	0	+ 249 ± 2
+ 1, − 1	+ 259 ± 2	*A*	+ 257 ± 2
A, *C*	+ 252 ± 2	*B*	+ 254 ± 2
B, *D*	+ 245 ± 2	+ 1	+ 250 ± 2
		C	+ 265 ± 2
		D	+ 262 ± 2
		− 1	+ 254 ± 2
weighted mean	+ 252 ± 3	weighted mean	+ 254 ± 2

The results are shown in Tables 5 and 6. The mean errors have been calculated by the method described in I. Because of its asymmetry, the centre profile of M33 was not used in calculating V_n.

The mean of the three final numbers of Table 5 gives for M33: $V_n = -176 \pm 2$ km/sec; the mean of the two final values in Table 6 gives for M101: $V_n = +253 \pm 3$ km/sec. Both results are in good accordance with the optical data (Table 4).

6. *Density distribution*

Our reduction method was to determine $J(x,y)$ from the observations, next to solve for q_0 and q_a, which are the average values of $N(a)$ in successive elliptical rings, by means of eq. (11).

M33. Only the observations on the major axis were used for the reduction. The half of the nebula with positive x and the half with negative x were reduced separately, making use of eqs (5), (6) and (12) and putting $V_1 = 0$ and $\varphi_1 = \pi/2$. The values of $J'(x) = J(x, 0)$ and $J''(x) = J(x) - J'(x)$ were found by measuring the areas of the profiles in Figure 1b left and right of the centre velocity and are represented in Table 7 under the head "observed". We took the rings of hydrogen situated at $a = 1, 2, 3$. Using equation (12), with $\rho = {}^1/_2$, we obtained a set of equations from which q_a could be solved:

$$J'(x) = \frac{\pi \sin i}{8\,\Omega'}\, q_0 f|x| + \sum_{a=1}^{\infty} q_a f'_x(a).$$

The values of q_a that were found to give the best solution, are given in Table 8. The corresponding values of $J'(x)$ and $J''(x)$ are entered as "computed" in Table 7. The column "model" in Tables 7 and 8 gives the average values of the computed $J(x)$ and q_a for the two halves. The density distribution so obtained is represented in Figure 6.

TABLE 7
M33

Emission by southern half				Emission by northern half				Model
$x(\frac{1}{4}°)$	1000 J' obs	1000 J' comp	diff	$x(\frac{1}{4}°)$	1000 J'' obs	1000 J'' comp	diff	1000 J
− 2	10[1]	4	2[1]	2	7	4	3	4
− 1	39	41	− 2	1	32	35	− 3	38
0	127	124	3	0	110	108	2	116
1	164	164	0	− 1	165	165	0	164
2	116	114	2	− 2	143[1]	137	0[1]	126
3	42	42	0	− 3	58	58	0	50
4	5	10	− 6	− 4	10	14	− 4	12

[1] These values refer to $x = -1.8$

TABLE 8
M33. Average densities in successive rings.
unit = 1 cm^{-3} kpc

a $(\frac{1}{4}°)$	q_a South	q_a North	Model
0	0.66	0.66	0.66
1	0.28	0.12	0.20
2	0.20	0.30	0.25
3	0.02	0.02	0.02

FIGURE 6

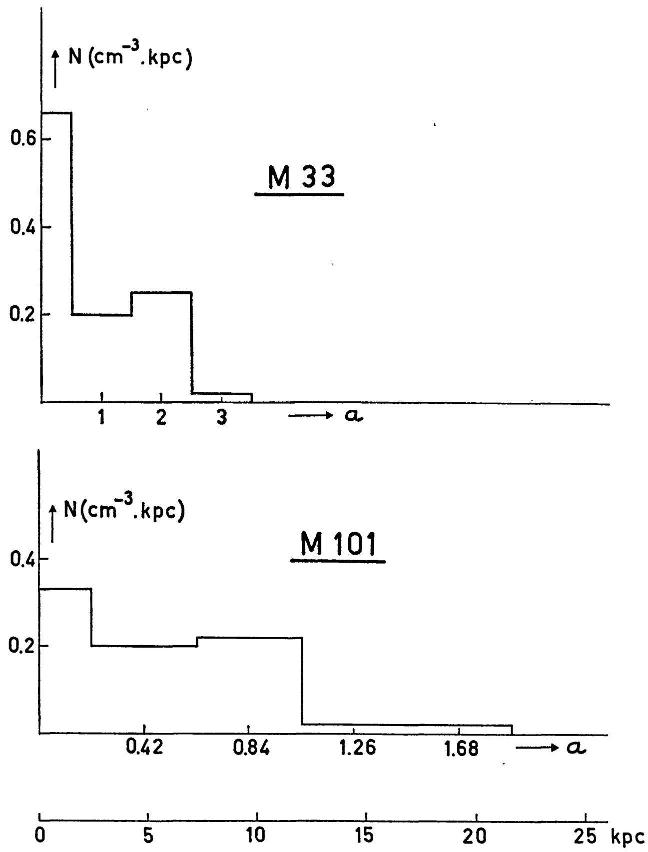

Density distribution in M33 and M101.

TABLE 9

M101

field	1000 $\mathcal{J}$ obs	comp	diff
0	105	105	0
+ 1	69	72	− 3
− 1	69		
+ 2	28	22	+ 6
− 2	28		
A	66	70	0
B	85		
C	62		
D	68		

TABLE 10

M101. Average densities in successive rings
unit = 1 cm^{-3} kpc

a (¼°)	q_a
0	0.33
0.42	0.20
0.84	0.22
1.26	0.02
1.68	0.02

M101. All observed profiles were used to derive the density distribution. Assuming symmetry, the profiles *A*, *B*, *C* and *D* should have the same value of $\mathcal{J}(x)$.

We took $\rho = 0.21$ in eq. (18) and solved for the q's. The results are shown in Tables 9 and 10.

7. *Rotation and model line profiles*

Model line profiles for both nebulae were calculated by means of eqs (6), (9) and (12) with the density distributions represented in Table 10 and in the column "model" of Table 8. The values of $V(a)$ that were found to give good agreement with the observed profiles are represented in Tables 11 and 12.

TABLE 11

M33. Rotational velocities

a (¼°)	$V(a)$ (km/sec)	Θ_{rot} (km/sec)
¼	50	60
1	86	102
2	84	100
3	82	98

TABLE 12

M101. Rotational velocities

a (¼°)	$V(a)$ (km/sec)	Θ_{rot} (km/sec)
0.10	60	132
0.42	80	176
0.84	80	176
1.26	80	176
1.68	80	176

The rotation curve of M33 is shown in Figure 7 together with optical data of MAYALL and ALLER (1942). The model line profiles (dashed curves in

FIGURE 7

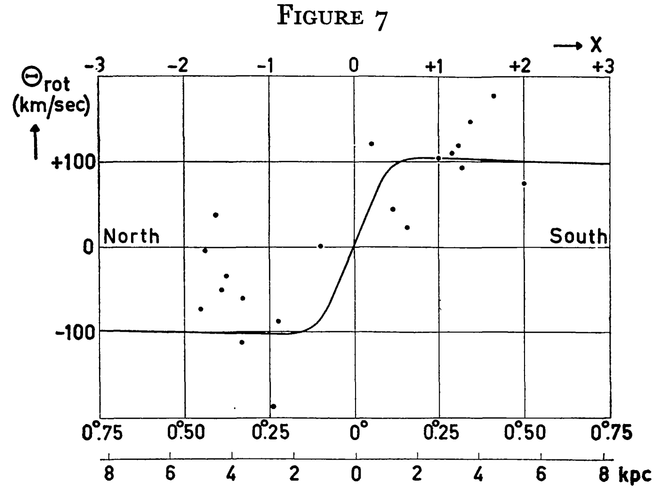

Rotation M33; dots are optical data.

Figures 1b and 2b) were calculated from eq. (9) by putting $\Delta V = 60$ km/sec. The profiles were computed for the observed points in the nebulae at intervals of 20 km/sec in V. Profiles calculated with $\Delta V = 40$ km/sec and $\Delta V = 80$ km/sec did not agree so well with the observations.

8. *Mass*

Using equations (10), (13) and (14) we derived the hydrogen mass and the total mass of the nebulae.

M33. Using the distance of $630\,c$ kpc, the unit of a in the previous section corresponds to $1/4° = 2.75\,c$ kpc, where c is a correction factor, which is supposed to be close to unity.

Eq. (13) gives:

$$\frac{M_{\rm H}}{m_{\rm H}} = 2\pi \times 0.84 \text{ cm}^{-3}\text{kpc } (1/4°)^2 = 2\pi \times 0.84 \times (2.75\,c)^2 \text{ cm}^{-3}.\text{kpc}^3.$$

Multiplying by $\left(\frac{m_{\rm H}}{M_\odot}\right)\left(\frac{1 \text{ kpc}}{1 \text{ cm}}\right)^3 = 2.47 \times 10^7$

we obtain $M_{\rm H} = 0.99 \times 10^9 c^2 M_\odot$.

The total mass is calculated by eq. (14); at $R = 0°.75 = 8.25\ c$ kpc, we have $\Theta_{rot} = 98$ km/sec and hence (assuming that we may take $k = 1$) we obtain

$$M = 18 \times 10^9\ c\ M_\odot.$$

The relative hydrogen mass of the nebula is

$$\frac{M_{\rm H}}{M} = 0.055\,c.$$

Using the apparent distance modulus $24^{\rm m}.1$ and the apparent total photographic magnitude $6^{\rm m}.19$ (Table 4) the luminosity is found to be

$$L = 1.7 \times 10^9\ c^2\ L_\odot,$$

and $$\frac{M}{L} = 11\ c^{-1}.$$

M101. Using the distance 2600 c kpc we find

$$M_{\rm H} = 2.98 \times 10^9\ c^2\ M_\odot.$$

Further from $R = 0°.42 = 19.22\ c$ kpc, $\Theta_{rot} = 176$ km/sec and $k = 1$,

$$M = 140 \times 10^9\,c M_\odot.$$

The ratio is

$$\frac{M_{\rm H}}{M} = 0.021\ c.$$

Using data from Table 4 we obtain

$$L = 10.5 \times 10^9\ c^2\ L_\odot,$$

and $$\frac{M}{L} = 13\ c^{-1}.$$

9. *Discussion of the results*

M33. The model curves would have fitted the observed ones slightly better if we had computed them separately for the two halves. The computed curve at $x = \pm 4$ is too high, so the value of q_a for $a = 4$ has to be somewhat lower. The radio nebula is not much bigger than the optical one. The asymmetry in the centre profile can only be explained by some asymmetry in the nebula. The agreement between observed and computed curves for the points on the minor axis is very good, considering the fact that these observations were not used in deriving the density distribution.

A change in the rotational velocity would cause a shift of the model profiles, so Θ_{rot} is probably correct within 5 km/sec. The rotation near the centre is of course uncertain.

An asymmetry in the rotation law can only be detected after model profiles have been calculated for the two halves of the nebula separately. However, the velocity differences between the two halves seem to be less than 7 km/sec.

The profiles $y = +1$ and $y = -1$ show a difference in V of 7 ± 4 km/sec. In case this should be due to a possible expansion in the inner part of the nebula, it would correspond to an expansion velocity of 4 ± 2.5 km/sec in the plane of the nebula. The NW-side of M33 then would be nearer to us.

The earlier estimate of the hydrogen mass (RAIMOND and VOLDERS 1957), when corrected for revised distance and intensity scale, is $0.8 \times 10^9 M_\odot < M_{\rm H} < 3.8 \times 10^9\ M_\odot$, in agreement with the present results.

M101. The dip in the centre profile depends very strongly on the rotational velocity in the rings near the centre. Thus the value of $V(a)$ in these rings is correct within a few km/sec. In the outer rings 1.26 and 1.68 the density and rotation are uncertain because of the very low intensities in the profiles $x = \pm 2$ and $x = \pm 3$. In our model we have assumed $V(a)$ to have the same value for all a; this assumption introduces an uncertainty of perhaps 20% in the calculation of the total mass.

We have assumed the effect of selfabsorption to be small. If this assumption is not correct, all densities would increase and a higher hydrogen mass would be found. However, the chance that there is considerable selfabsorption is even smaller than for M31.

ACKNOWLEDGEMENTS

I would like to thank Prof. H. C. VAN DE HULST, Prof. J. H. OORT and Mr H. VAN WOERDEN, with whom I had many helpful discussions and who were always ready to advise me in many difficulties. I also acknowledge discussions with Dr M. SCHMIDT, Dr G. WESTERHOUT and Mr G. W. ROUGOOR.